

A person in a dark sweater and blue jeans stands in a large industrial facility, likely a wind tunnel. They are positioned behind a large black camera mounted on a tripod, which is aimed at a large, light-colored aerodynamic model. The person is also looking at a laptop screen on a black equipment case to their right. The background shows the interior of the wind tunnel with various structural elements and lighting.

# Review of aeronautical fatigue and structural integrity investigations in the Netherlands during the period March 2023 - March 2025

# **Review of aeronautical fatigue and structural integrity investigations in the Netherlands during the period March 2023 - March 2025**

R.C. Alderliesten

## **Abstract**

This report is a review of the aeronautical fatigue and structural integrity activities in the Netherlands during the period March 2023 to March 2025. The review is the Netherlands National Delegate's contribution to the 39<sup>th</sup> Conference of the International Committee on Aeronautical Fatigue and Structural Integrity (ICAF) in Xi'an, China, on 9 to 12 June 2025, and published on the ICAF website in June 2025.

## Table of Contents

Abbreviations .....	4
1. Introduction .....	5
2. Metal Fatigue .....	6
2.1. Prediction of fatigue in engineering alloys – part 2 (PROF-2).....	6
2.2. Cold Spray Research.....	8
3. Bonded Structures .....	9
3.1. Sustainable Structural Bonding Technologies (SUBSONIC).....	9
4. Composites .....	10
4.1. High-cycle fatigue of propeller blades .....	10
4.2. Large damage capability of thermoplastic orthogrid fuselage .....	10
4.3. Thermoplastic Composites - Fatigue, Damage tolerance and Durability .....	12
4.4. Fatigue After Impact .....	13
4.5. Planar delamination .....	14
4.6. D-STANDART Project.....	14
4.7. Determination of Mode I Fatigue Delamination Propagation in Unidirectional Fibre-Reinforced Polymer Composites.....	16
4.8. Static and Fatigue Mode I Delamination Propagation in Thermoplastic Composites .....	16
5. Probabilistic Modelling & Risk Analysis .....	18
5.1. Bayesian Inference for updating EIDS distributions in probabilistic crack growth.....	18
6. Non-Destructive Evaluation .....	21
6.1. Development of Non-Destructive Inspection techniques for large scale parts at NLR .....	21
6.2. Development and evaluation of Laser Ultrasonic Inspection at NLR .....	22
7. Structural Health & Usage Monitoring .....	24
7.1. SHM for LH2 tank applications.....	24
8. Fleet Life Management .....	26
8.1. Individual tracking of RNLAf aircraft .....	26
References.....	27

## Abbreviations

CFRP	Carbon fibre reinforced polymer composites
DCB	Double Cantilever Beam
FCG	Fatigue Crack Growth
PROF	PRediction Of Fatigue in engineering alloys
RNLAF	Royal Netherlands Air Force
SHM	Structural Health Monitoring
VA	Variable Amplitude

## 1. Introduction

The present report provides an overview of the work and research performed in the Netherlands in the field of aeronautical fatigue and structural integrity during the period from March 2023 until March 2025. The subjects in this review come from the following contributors:

- Delft University of Technology (TUD)
- GKN Aerospace-Fokker (GKN Fokker)
- Royal Netherlands Aerospace Centre (NLR)
- Royal Netherlands Air Force (RNLAf)
- University of Twente (UT)

Additionally, collaborative work between the NLR and the Defence Science and technology Group (DST-G) of Australia, and between TU Delft and various European universities and institutes is included.

The names of the principal investigators and their affiliations are provided at the start of each subject. The format and arrangement of this review is similar to that of previous national reviews.

## 2. Metal Fatigue

### 2.1. Prediction of fatigue in engineering alloys – part 2 (PROF-2)

*Emiel Amsterdam (NLR)*

The PROF-2 project is a five year Public Private Partnership between NLR, C-TEC Constellium Technology Center, Lagerwey, RUAG, Korea Aerospace Industries, GKN Fokker, Airbus and the Ministry of Defense. The objective of the project is to develop a unified probabilistic fatigue life assessment framework. In PROF-2 knowledge of the fatigue crack growth rate (FCGR) of long and small cracks and their distribution will be gained and used to create a unified probabilistic fatigue life assessment framework that allows determining the life distribution of a structure for a given initial discontinuity size distribution or rogue flaw size. The proof of concept of the new theoretical framework from the initial PROF project will be extended to create a cycle-by-cycle model to predict VA crack growth for any given variable amplitude (VA) loading spectrum.

For positive stress ratios it was proven that the fatigue crack growth rate ( $da/dN$ ) shows a power law relationship with the cyclic strain energy release rate ( $\Delta G$ ) over the maximum stress intensity factor ( $K_{max}$ ):

$$\frac{da}{dN} = C \left( \frac{\Delta G}{K_{max}} \right)^n = C \left( \frac{(1 - R^2) K_{max}}{E} \right)^n \quad (1)$$

where  $C$  and  $n$  are material constants,  $R$  is the stress ratio and  $E$  the Young's modulus. The  $1/K_{max}$  term in Eq. 1 is related to the residual stress field from the plastic zone at the crack tip. Crack retardation can be incorporated in the model by relating the  $1/K_{max}$  term to the  $K_{max}$  of the overload and calculating  $\Delta G$  based on the  $K_{max}$  and  $K_{min}$  of the cycles after the overload. Under the assumption that a variable amplitude spectrum is repeated often and the crack does not grow out of the residual stress field of the maximum spectrum stress, the fatigue severity index (FSI) of a spectrum can be calculated using the following equation:

$$FSI = \frac{1}{f} \sum_{t=1}^f |R_t^2 - R_{t-1}^2|^n \quad (2)$$

where  $f$  is the number of turning points and  $R_t$  the turning point stress ratio of the normalized spectrum. The FSI is 1 for constant amplitude (CA) loading with  $R=0$ . It has been shown that the average fatigue crack growth rate under variable amplitude loading has a linear relationship with the FSI [1]. Integrating the fatigue crack growth from the initial to the final crack length gives the crack growth life ( $N_{CG}$ ), which is dependent on the FSI of a normalized spectrum and maximum spectrum stress ( $S_{MSS}$ ) that is used to scale that spectrum:

$$N_{CG} = \frac{C^*}{FSI} S_{MSS}^{-n} \quad (3)$$

where  $C^*$  is dependent on the material, specimen geometry and the initial and final crack length. Multiplying both sides with the FSI should result in an  $S$ - $N_{CG}$  curve for VA loading that falls on top of the  $S$ - $N_{CG}$  curve for  $R=0$  (since the FSI is 1 for  $R=0$ ) [2]. Figure 1 shows the  $S$ - $N_{CG}$  curve for middle tension (M(T)) specimens loaded with CA and various VA spectra. All curves fall on top of each other and create a master curve for this material, specimen geometry and the initial and final crack length. However, Figure 2 shows that the same applies for another material and specimen geometry that

represents a structural element and where the fatigue cracks nucleate from inherent discontinuities that are present in the material.

This shows that the fatigue life of a random spectrum and random structural element can be related to the fatigue life of that structural element for a known spectrum by the difference in energy between the two normalized spectra. The effect of the magnitude of the spectrum is incorporated in the  $S-N$  curve. Hence, the fatigue life for any given stress spectrum can be reliably calculated with the present methodology. This can, for example, be used to determine the VA fatigue life of different locations in a digital twin, where each structural element has its own stress spectrum and magnitude.

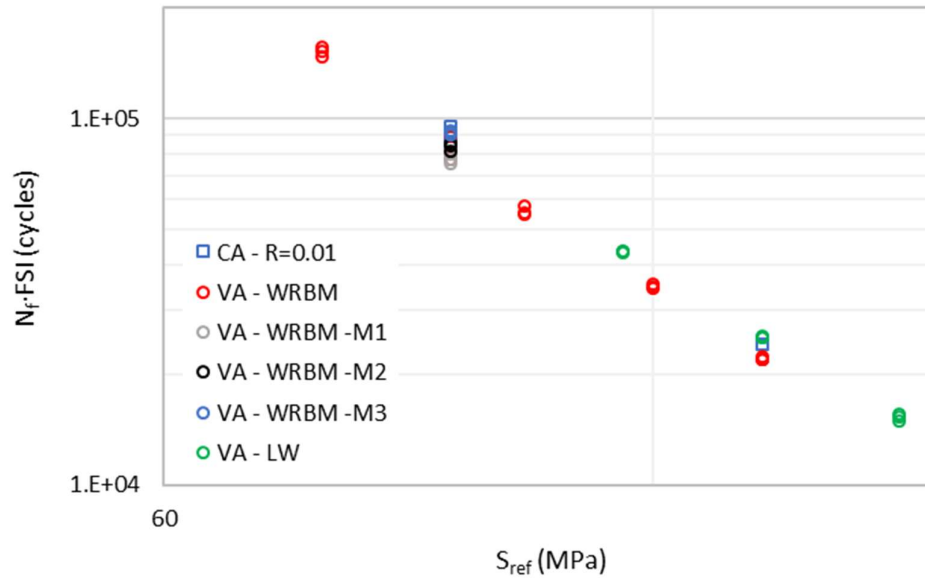


Figure 1 Fatigue crack growth life times the FSI as a function of the reference stress (MSS for VA and  $S_{max}$  for CA loading, respectively) for M(T) specimens loaded with CA and various VA spectra

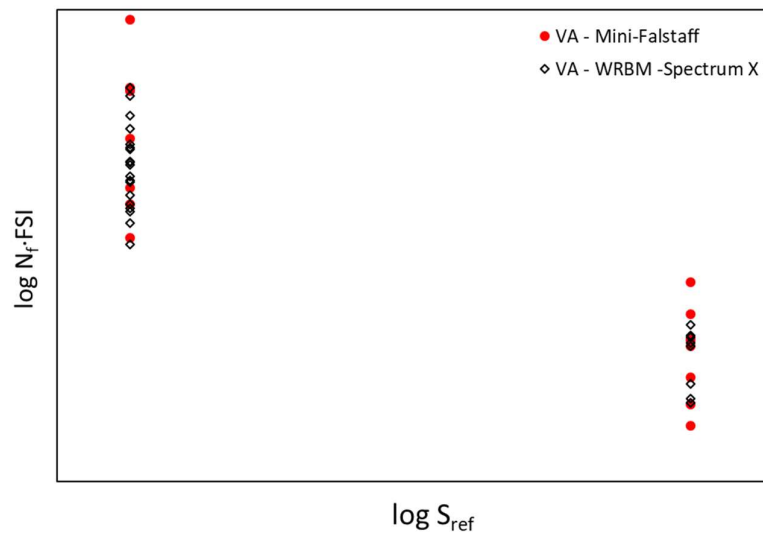


Figure 2 Fatigue life times the FSI as a function of the reference stress (MSS for VA) on a log-log scale for two different VA spectra. The first spectrum is mini-Falstaff and the other spectrum is a WRBM spectrum with a significantly different severity. The specimens consisted of strips of an aerospace grade aluminium with a hole in the centre. The specimens exactly followed the same hole drilling and surface finish process as the actual aircraft (anodising and primer).



## 2.2. Cold Spray Research

*Mary Patrick, Stratos Koufis, Margot van Hecking Colenbrander, John-Alan Pascoe (TUD)*

Cold Spray is an emerging metal deposition technology which can be used for the repair of aerospace structures. Currently research into the application of this technology is underway at TU Delft within the context of two projects.

In the Brightsky project TU Delft, NLR, Amsterdam University of Applied Sciences, EPCOR, and KLM Engineering & Maintenance are collaborating on the qualification of cold spray as a repair technology for civil aircraft components. In addition, Stratos Koufis (TU Delft) is investigating the use of airborne acoustic emissions to monitor the process as a tool for quality assurance. The first proof of concept was published in [3].

In the CSAR project, funded by the Dutch Research Council Open Technology Programme, Mary Patrick (TU Delft) is investigating the fatigue performance of cold spray repairs, with the aim of developing a prediction methodology and Margot van Hecking Colenbrander is investigating the impact resistance of cold spray.

Thanks to a collaboration with EPCOR, a Titomic D623 cold spray system was installed at TU Delft in summer 2024, allowing for intensification of the research activities. A similar system was installed at the Perron 038 research centre in Zwolle.



*Figure 3 Cold spray machine in action at TU Delft.*



### 3. Bonded Structures

#### 3.1. Sustainable Structural Bonding Technologies (SUBSONIC)

*Ishan Manoj, René Alderliesten, John-Alan Pascoe (TUD), Christine Obbink-Huizer, Marc van der Geest, Jan Waleson, Bas Tijs (GKN Fokker)*

Within the Dutch National program Top Sector High Tech Aircraft manufacturing technology (TSH) a collaborative program between GKN Fokker and TU Delft has been granted to develop novel methodologies for structural adhesive bonding compliant to the more stringent certification requirements concerning fatigue and damage tolerance. In addition the project aims at broadening the application of structural adhesive bonding by facilitating further development of structural bonding process and automation of it. The project runs until the end of 2027, and more results are expected to be reported in the next national review.

## 4. Composites

### 4.1. High-cycle fatigue of propeller blades

*Ruben Nahuis and Tim Panis (NLR)*

Within the EU-sponsored Clean Aviation technology program HEROPS (Hydrogen-Electric Zero Emission Propulsion System), NLR contributes to the development and validation of a 2-4 MW liquid hydrogen powered propulsion system, with a focus on the design of a new propeller suitable for this. NLR will actually build and test this propeller on a model scale. Given the typically high fluctuating loads for propellers in combination with high speeds for this type of carbon composite blades on a scale, many millions of highly loaded changes of the laminate easily take place. In this program, high-cycle fatigue (HCF) for model blades is investigated and an attempt is made to understand the development of damage for a typical model blade laminate and to investigate the effect of this on its natural frequency/ phase. Test elements have now been made and are currently being used for HCF testing and inspections. Each element is vibrated at a fixed amplitude at its natural frequency and this typically lasts millions of cycles until a fixed decrease in natural frequency/phase is observed. After each step, the element is examined for damage and then further tested. See Figure 4 showing the laminate on one of NLR's shakers.

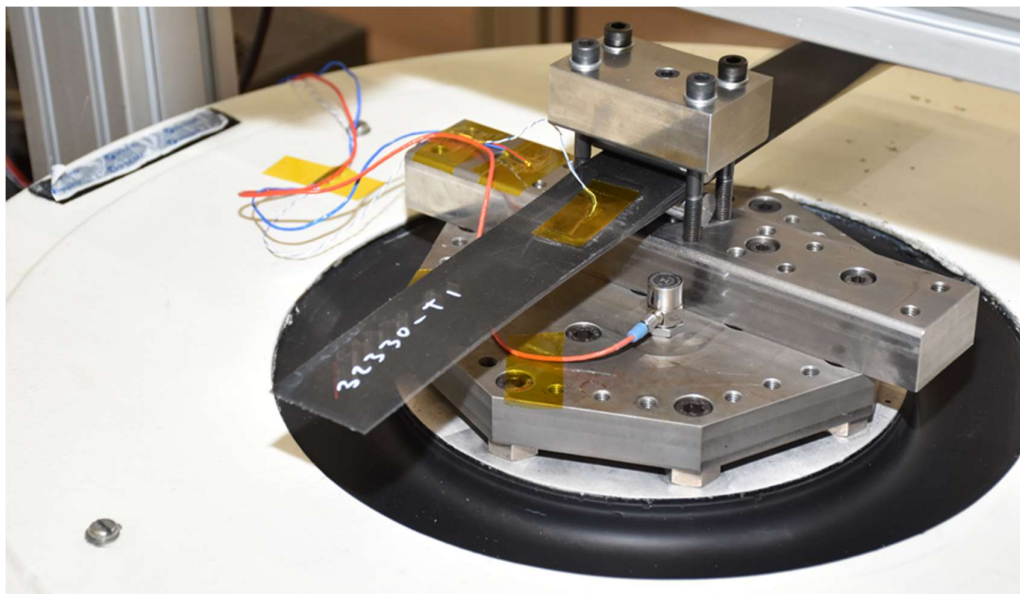


*Figure 4 HCF test of a composite laminate on a shaker.*

### 4.2. Large damage capability of thermoplastic orthogrid fuselage

*Jan E.A. Waleson and Jaap Willem van Ingen (GKN Fokker)*

As presented in 2023, an integral, carbon fibre reinforced thermoplastic orthogrid structure is proposed as a light, cost competitive option for a non-pressurized, double curved aft fuselage structure of a business jet. See Figure 5 and [4]. Drag reduction using the area rule for the fuselage between the engines led to the double curved shape, which is more easily realized in composites. The structure consists of a co-consolidated skin, laid up by automated fibre placement, and flat pre-

forms for the frames and stringers. The joints that are mainly loaded in shear are made by means of short-fibre fillets in so-called “butt joints” and conduction welding.

Damage tolerance of this disruptive, highly integrated thermoplastic fuselage structure was assessed using Advisory Circular AC20-107B [5], as conclusive approach. No showstoppers were found in the extensive work.



*Figure 5 New stiffened fuselage panel concept without mechanical fasteners.*

For two-bay skin cracks including one severed stiffener in metal fuselage designs, arrest at the adjacent stiffeners is often ensured as extra layer of safety. This so-called structural damage capability is at the discretion of the OEM. However, since composite designs should afford the same level of fail-safe, multiple load path structure assurance as conventional metals design [5], the aft fuselage was designed for arrest of a large notch (two half bays) with a severed stringer. The onset of growth halfway between the stringers allowed for the development of crack tip blunting by delaminations in the skin laminate.

To enhance the residual strength, four local plies in the stringer lengthwise direction were interleaved in the 14-ply skin layup. The large notch was tested in tension in a 6-stringer panel of three frame bays at NLR. See Figure 6.



*Figure 6 Final failure in tension of the stiffened panel with large notch. Courtesy NLR.*

Onset in the 14-ply skin layup occurred at 281 kN. At 645 kN, both crack tips had reached the interleaved tear straps below the adjacent stringers. The maximum load that was reached was 794 kN, which showed that the tear straps ensured effective arrest of large notches.

In order to predict the required number of tear strap plies for other skin layups, correlation with several analysis approaches is ongoing.

### 4.3. Thermoplastic Composites - Fatigue, Damage tolerance and Durability

*Sofia Sartorio, René Alderliesten, John-Alan Pascoe (TUD)*

This research is embedded in the large LIT project which stands for Luchtvaart in Transitie. The goal of this initiative is to contribute to the development of more sustainable aviation. In this framework, this specific project focuses on the fatigue behaviour of thermoplastic composites. The large number of models present in literature to predict this phenomenon use fitting variables that lack physical meaning, losing the connection between the physics and the prediction.

Therefore, this project aims at developing a physics-based model to predict the fatigue behaviour of thermoplastic composites. To achieve this, the link to the physics will be established, considering the energy dissipated by specific damage mechanisms. The variable, at the core of this model, that should be able to characterize the dissipative mechanisms, is the ratio between the total dissipated energy (sum of hysteresis cycles until failure) and the total applied work. In addition to obtaining a model that can be applied broadly, the effect of temperature, frequency, stress ratio, and fibre orientations will also be incorporated.

With this aim, Polyetherketoneketone Carbon Fibre Reinforce (PEKK-CF) samples with 16 layers with different fibre orientations were tested both under tensile-tensile fatigue loading for different stress levels and quasi-static loading. From these tests, the ratio previously described was calculated and the results were reported in Figure 7. As shown in Figure 7 three main ratios are present. The first one applies to angle-ply composites, where dissipation is matrix-dominated. The second is valid for unidirectional composites with fibres parallel to the load application, where dissipation is fibre-dominated. The third ratio is characteristic for both unidirectional composites with fibres perpendicular to the load direction and cross-ply composites, where the dissipative mechanism involves failure at the fibre-matrix interphase. The ratios resulting from quasi-static tensile tests follow a similar trend, but the values are slightly higher. For this reason, additional investigation to correlate fatigue and static tests is needed. In addition, the ultimate fatigue strain appears to be proportional to the ratio between the applied stress level and the ultimate tensile strength (Figure 7). This is another interesting takeaway that should be properly investigated in future research. The next step will be to introduce this ratio in the modelling of the fatigue behaviour.

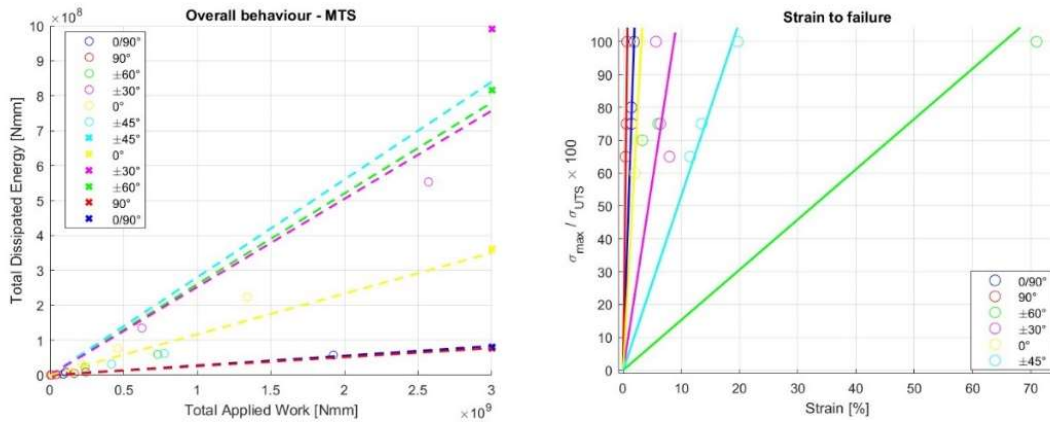


Figure 7 Total Dissipated Energy vs Total applied work for different fibre orientations. Circles represent data from fatigue tests at various stress levels. Crosses represent data from quasi-static tensile tests (left); Strain to failure for different stress levels and fibre orientations (right)

#### 4.4. Fatigue After Impact

Davide Biagini, John-Alan Pascoe (TUD)

Davide Biagini conducted a PhD thesis on the topic of fatigue after impact; some results of which were presented at ICAF 2023. His research showed that the ‘delamination growth plateau’ sometimes reported in the literature can be the result of limitations of the applied non-destructive inspection technologies, rather than a physical effect. E.g. shorter surface level or delaminations (such as visible in Figure 8) may be continually growing, without resulting in the growth of the overall projected delamination area. Biagini also developed a machine learning approach to classify acoustic emission signals and thereby analyse the activity of different failure mechanisms throughout both quasi-static loading to failure and a fatigue life. Biagini’s thesis is publicly available [6].

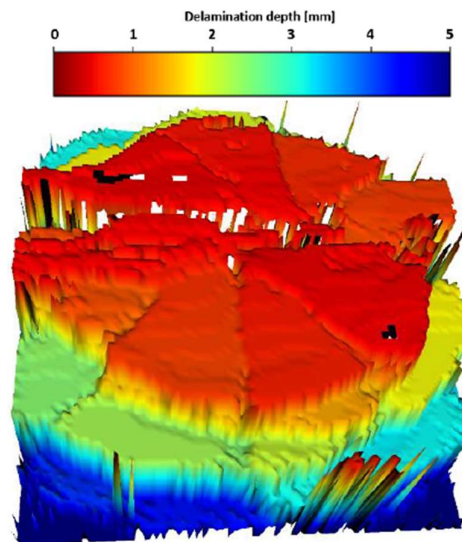


Figure 8 Ultrasonic scan of impact damage in a CFRP laminate - Biagini et al., ICAF 2023

#### 4.5. Planar delamination

Wenjie Tu, John-Alan Pascoe (TUD)

Wenjie Tu is conducting a PhD thesis on the topic of planar delamination growth. The current practice for characterizing delamination growth is to make use of beam-shaped specimens, where the delamination growth is assumed to be essentially one-dimensional. However, in operational structures, delaminations will likely grow in a two-dimensional manner. Tu developed a test set-up to create planar delamination growth in a square specimen loaded by out of plane compression (presented at ICAF 2023). It was observed that the delamination immediately migrates (Figure 9) until the local fibre orientation matches the delamination growth direction. Tu's work has continued to examine the similarities and differences between beam-shaped coupon specimens and planar delamination growth specimens, as well as the effect of lay-up on the delamination growth behaviour. The latter was recently published in open access [7].

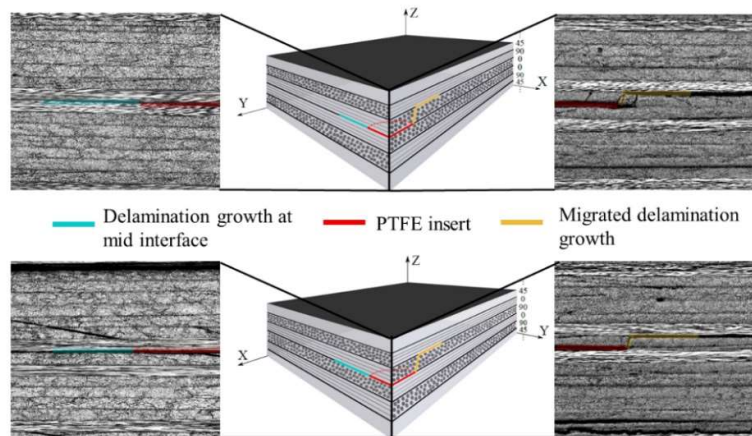


Figure 9 Delamination migration during planar delamination growth, Tu et al., ICAF 2023

#### 4.6. D-STANDART Project

Francisco Monticeli, John-Alan Pascoe (TUD), Dario di Maio, Jordy Schönthaler, Matias Lasen, Friso Oude Tanke (UT), Marco Nawijn (NLR)

The D-STANDART Project aims to improve the evaluation of the fatigue behaviour of full scale composite structures, by developing both novel experimental approaches, as well as making use of AI-enabled surrogate modelling to capture the effects of fibre lay-up and manufacturing defects, while keeping the computational cost low enough to analyse full-scale structures in industry-scale analyses.

The D-STANDART consortium is led by the Netherlands Aerospace Centre (NLR, Marco Nawijn) and is further comprised of: University of Twente, TU Delft, Hexagon, L-UP, Suzlon, University of Bristol, National Composites Centre and iCOMAT.

Within the Netherlands, the University of Twente (Dario di Maio, Jordy Schönthaler, Matias Lasen, Friso Oude Tanke) focused on developing a high frequency test method that enables material screening and the identification of delamination onset within hours rather than days. TU Delft investigated the effects of fibre orientation and environment on fatigue delamination growth



(Francisco Monticeli, Xi Li, Davide Biagini, Yasmine Mosleh, John-Alan Pascoe), as well as working on the surrogate modelling approach (Georgios Soimouris, Vahid Yaghoubi, Boyang Chen). NLR assisted in the delamination growth characterization (Emiel Amsterdam, Robbert-Jan van den Brink) as well as full scale modelling of element level demonstrator tests (Niels van Hoorn, Wouter van den Brink, Farid Talagani) that will be conducted in the final part of the project.

XCTE is one of the Key Exploitation Results of the D-STANDART project. XCTE's vision and mission focus on integrating composite durability characterization and dynamic response analysis to enhance system resilience. Our mission aligns with industry needs in this critical capability area.

Understanding material behaviour and its response is essential to developing stronger, more resilient, and lightweight structures.

Material durability is assessed through high-frequency fatigue testing — an innovative method that dramatically reduces the time required to obtain fatigue data, from weeks to a few hours. This accelerated assessment leverages a physical principle that amplifies small variations in dynamic stiffness, enabling the detection of microscopic fatigue damage at its earliest stages. The combined testing and analysis techniques generate material master curves for both coupon and component laminates.

Early damage onset detection not only shortens testing durations, but also provides essential input for dynamic response simulations. These simulations allow engineers to predict vibration amplification linked to specific damage levels, empowering more informed design decisions. By uncovering the relationship between damage progression and dynamic behaviour, XCTE's technologies expand the design space beyond traditional zero-damage tolerance criteria, unlocking new possibilities for optimized and resilient systems.

XCTE addresses two primary shortfalls in the current design workflow for composite structures. The first is the prolonged testing time required to generate fatigue data. XCTE's high-frequency vibration fatigue testing accelerates data acquisition, delivering results in hours rather than weeks. This breakthrough enables near real-time data streams, supporting engineers in material and structural optimization.

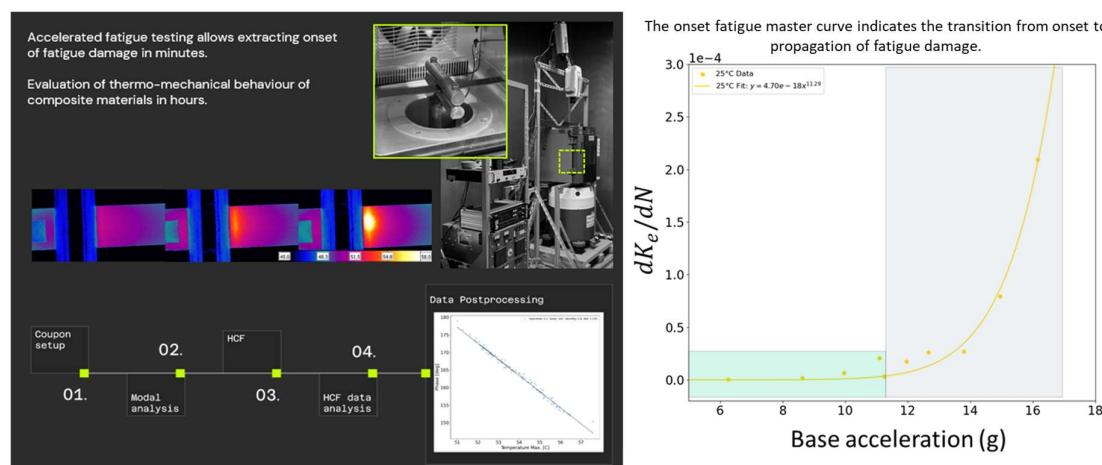


Figure 10 Illustration of the accelerated fatigue testing method developed at UT

The project is currently in its final year. Some results have already been published, including two journal papers by [Li et al.](#) [8] and [Monticeli et al.](#) [9]. Further publications are foreseen throughout 2025 and perhaps 2026. This includes the publication of an extensive fatigue characterization of



IM7/8552 carbon/epoxy composite. All D-STANDART related publications can be accessed via the website: <https://d-standart.eu/>

In addition to the publications and datasets, the D-STANDART consortium has also developed a series of online training materials on fatigue of composites, which are accessible via the D-STANDART Academy page on the D-STANDART website: <https://d-standart.eu/d-standart-academy/>

#### 4.7. Determination of Mode I Fatigue Delamination Propagation in Unidirectional Fibre-Reinforced Polymer Composites

*René Alderliesten (TUD), Andreas Brunner (empa)*

Although that standardized test methods are available to characterise quasi-static mode-I delamination fracture toughness (ISO 15024) and the fatigue delamination onset (ASTM D 6115), fatigue delamination propagation has not been standardized yet. Despite several initiatives and round robin exercises, no consensus has been achieved on how to evaluate the fatigue growth, in particular when large scale fibre bridging occurs.

This fibre bridging is generally attributed to the unidirectional lay-up adopted in the Double Cantilever Beam (DCB) specimen, which artificially increases the delamination resistance. This in most cases results in unconservative data, because the amount of fibre-bridging in structural applications is generally limited or even absent. Hence, for design, a "conservative" value is desirable. Quantifying the effects of fibre-bridging on delamination propagation in unidirectional laminates would allow for estimating the intrinsic delamination resistance and corresponding scatter of this laminate, satisfying the safety factor requirements defined in design guidelines.

To this aim, a test procedure is in development within ESIS-TC4 describing an experimental procedure to quantify and exclude the contribution of large-scale fibre bridging in mode I fatigue fracture tests of unidirectionally fibre-reinforced plastic composites. This test procedure comprises performing multiple sequences per specimen, to enable the derivation of a zero-bridging delamination resistance curve via regression through and translation of all data. This test procedure is a modification and extension of a former ESIS-TC4 test procedure, but also incorporates an analysis based on a modified Hartman-Schijve equation for the determination of scatter in the fatigue fracture curves (essentially  $da/dN$  versus a " $\sqrt{\Delta G}$ " related quantity instead of the "conventional" Paris-equation correlating  $da/dN$  with  $\Delta K$  or  $\Delta G$ ). To demonstrate the repeatability and reproducibility of the test procedure, a round robin exercise is currently executed with participants of the ESIS-TC4 committee, but also other parties are invited to participate.

#### 4.8. Static and Fatigue Mode I Delamination Propagation in Thermoplastic Composites

*Bas Tijs (GKN Fokker), Leciñana, Carreras, Renart, Zurbitu, Turon (UG)*

In collaboration with the university of Girona, Spain, several studies have been conducted to evaluate and assess mode I delamination in thermoplastic composites under static and fatigue loading conditions. The first study characterized the fatigue onset and propagation interlaminar properties of AS4D/PEKK-FC thermoplastic composite under mode I loading [10]. To reduce testing costs, a multi-fatigue testing rig capable of loading six specimens simultaneously was used. The offset observed in fatigue crack growth rate curves at different severities was attributed to fatigue R-curve effects and

was modeled using superposed fatigue cohesive laws. Various approaches to accounting for fatigue damage were compared with experimental data, providing insights into fatigue damage evolution. This led to the development of a novel modeling strategy based on a robust method for identifying fatigue model parameters in delamination scenarios where multiple failure mechanisms interact.

The second study introduced a delamination benchmark test concept for composite materials exhibiting non-self-similar delamination in characterization specimens [11]. This non-self-similar behavior is induced by rotating the loading blocks. The test's simplicity enables the analysis of loading mode history by combining various loading conditions, including static and fatigue loading, across multiple modes. The proposed methodology can be adapted to any composite material system and any sequence of loading conditions.

To demonstrate the test's capabilities, a case study is presented using AS4D/PEKK-FC thermoplastic composite, known for its strong R-curve behavior. A sequence of opening and shear failure modes was applied under static and fatigue loading, generating an experimental dataset for validating numerical delamination models. The delamination process was monitored using X-ray radiography, while final fracture surfaces were analyzed with scanning electron microscopy (SEM), providing physical insights into the role of fracture mechanisms in the delamination process

The third study assessed the effectiveness of cohesive zone modeling (CZM)-based approaches in predicting delamination in composite materials with large process zones under complex loading conditions [12]. The analysis focuses on R-curve effects under static and fatigue loading across multiple modes while accounting for loading history. To evaluate predictive capabilities, a state-of-the-art CZM-based simulation strategy is tested through a blind simulation of a validation benchmark. This benchmark promotes a non-self-similar delamination scenario, featuring an evolving process zone influenced by varying loading modes and a non-straight leading delamination front. The results demonstrate high accuracy in delamination prediction. Additionally, the relationship between the simulation strategy's features and the underlying delamination physics is explored. Special attention is given to the challenges of modeling an evolving process zone influenced by loading mode history.

## 5. Probabilistic Modelling & Risk Analysis

### 5.1. Bayesian Inference for updating EIDS distributions in probabilistic crack growth

*Paul Stuiver and Frank Grooteman (NLR)*

Structural risk analysis outcomes are largely driven by the equivalent initial damage size (EIDS) distribution which models the distribution of a hypothetical size of a pre-existing crack. An accurate representation of the EIDS distribution is crucial for reliable failure metrics. The goal of this research is to obtain a more accurate EIDS distribution from test and inspection data using Bayesian Inference, then fitting a distribution to backward calculated initial damage data.

The Bayesian Inference methodology offers a robust and flexible statistical framework by incorporating prior knowledge, inspection data and various sources of uncertainty. Let  $\theta$  represent the vector of parameters describing the EIDS distribution and  $\mathbf{D}$  the set of inspection data, which contains both detected and missed data points. The Bayesian formula the fundamental equation used and expressed by

$$p^+(\theta|\mathbf{D}) = \frac{L(\mathbf{D}|\theta) \cdot p^-(\theta)}{p(\mathbf{D})}$$

where

$p^-(\theta)$  is the prior, which represents the prior beliefs about  $\theta$ ,

$L(\mathbf{D}|\theta)$  is the likelihood, which represents how likely it is we observe the inspection data  $\mathbf{D}$  given  $\theta$ ,

$p^+(\theta|\mathbf{D})$  is the posterior, which represents the updated beliefs about  $\theta$  and

$p(\mathbf{D})$  is a normalization factor.

Note, that the posterior is a probability density function (PDF) of  $\theta$ . This means we can quantify the uncertainty by providing a range of possible values.

A numerical example has been worked out to update the EIDS distribution under the assumption that the EIDS distribution is given by  $a_0 \sim \text{Lognormal}(\mu, \sigma^2)$ , so that  $\theta = [\mu, \sigma]$ . The inspection data is generated with a probability of detection so that data points can be missed. Figure 11 and Figure 12 show that the maximum likelihood estimate of the posterior distribution yields a posterior EIDS that is substantially closer to the true EIDS distribution for 25 inspection data points.

In the first numerical example, a grid-based method was used by iterating over all possible parameter locations  $(\mu, \sigma)$ . This can become computationally expensive. In contrast, Markov Chain Monte Carlo (MCMC) methods navigate through the parameter space in a probabilistic manner by concentrating on parameter locations with significant posterior values, avoiding iterating over all possible parameter locations. Figure 13 shows the result of the same numerical example but using a MCMC method.

Since the MCMC method is much more efficient than Bayesian inference it is better suited to solve problems taking into account other uncertain sources like variability in crack growth material properties and loads. Another application is for instance mixed distribution functions. The

representation of the EIDS can be extended by incorporating a separate distribution for Rogue Flaws. In this case, the EIDS distribution becomes a mixture model given by

$$f(a_0; \mu_{IC}, \sigma_{IC}, \mu_{RF}, \sigma_{RF}, w) = w \cdot f_{IC}(a_0; \mu_{IC}, \sigma_{IC}) + (1 - w) \cdot f_{RF}(a_0; \mu_{RF}, \sigma_{RF}),$$

where  $f_{IC}$  is the initial crack distribution and  $f_{RF}$  the Rogue Flaw distribution and  $w \in [0,1]$ . In this case  $\theta$  becomes a five-dimensional vector. Here, using a grid-based method becomes infeasible and an MCMC method is much more appropriate. Figure 14 shows the results of a Bayesian Inference problem for the mixture model.

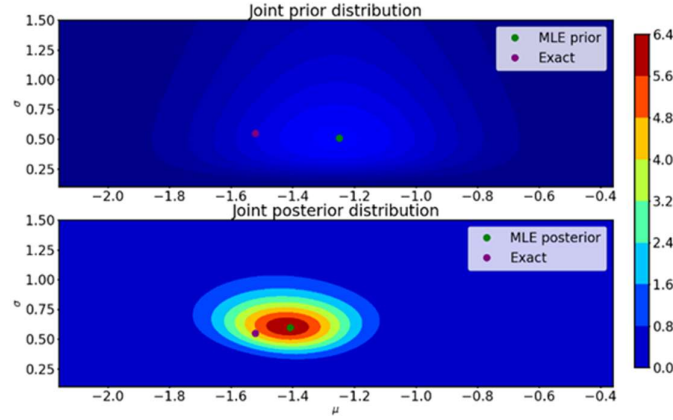


Figure 11 Joint prior (top) and posterior distribution (bottom) of  $\theta$ . The green dot represents the Maximum Likelihood Estimate of the prior (top) and posterior (bottom). The joint posterior is significantly closer to the exact lognormal parameters given by the purple dot.

For future research, there are two key areas of focus. Firstly, to improve the performance of the MCMC method by exploring alternative algorithms and implementing adaptive step size techniques. Secondly, to enhance the model's relevance and accuracy, with the aim to incorporate more complex crack growth models that use additional uncertainties and bridge the gap to real-world applications by validating our approach from practical scenarios. Furthermore, a comparison with the backward calculation method will be made.

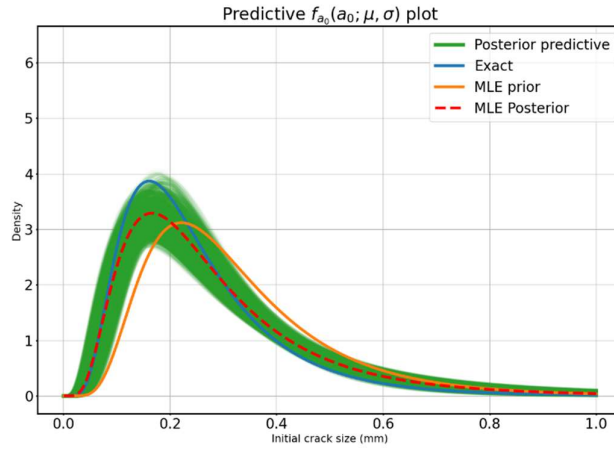


Figure 12 The predictive plot displays EIDS distributions obtained using the MLE prior model parameters (orange), MLE posterior model parameters (red) and the exact model parameters (blue) corresponding to the first numerical example. The green EIDS distributions show the variability in the posterior predictions.

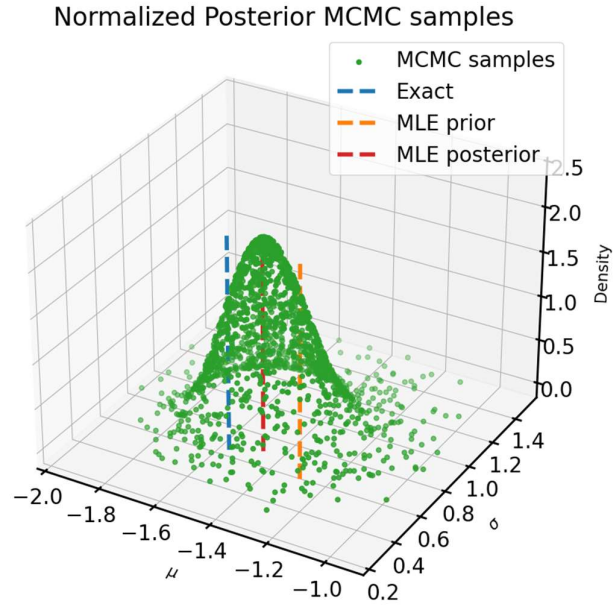


Figure 13 Normalized posterior MCMC samples (green) together with the exact, MLE prior and MLE posterior model parameters. Similar results to the grid-based method are obtained but with fewer samples.

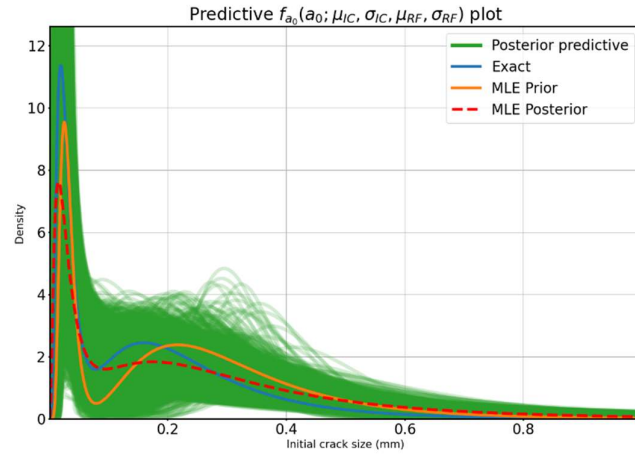


Figure 14 The predictive plot displays EIDS distributions obtained using the MLE prior model parameters (orange), MLE posterior model parameters (red) and the exact model parameters (blue) for the mixture model. The green EIDS distributions show the variability in the posterior predictions.

## 6. Non-Destructive Evaluation

### 6.1. Development of Non-Destructive Inspection techniques for large scale parts at NLR

*Daniella Deutz, Arnoud Bosch, Dion Baptista, Erik van Veen, Patrick Jansen, Jacco Platenkam (NLR)*

The production of large carbon-fibre reinforced polymer (CFRP) aircraft parts is a complex process where defects can have significant consequences. Ensuring precision and quality control is challenging due to the intricate nature of these components, resulting in scrap rates of up to 20%. Current quality control systems lack fast and automated inspection capabilities, allowing defects to propagate to later stages of production.

NLR has an extensive track record on non-contact Non-Destructive Inspection (NDI) methods based on optical sensors, such as 3D surface scanning, infrared thermography (IRT) and laser shearography for the detection of defects in composite parts [13]. By combining these methods, the structural integrity of an aircraft's outer surface can be quickly assessed, reducing inspection costs and downtime during production and maintenance. Figure 15 shows the demonstration of this concept, gathered as part of the FasterH2 EU project. Here the overlap joint of the Multifunctional Fuselage Demonstrator (MFFD), an 8 m long by 4 m diameter thermoplastic CFRP part, manufactured under the lead of Airbus [14] is inspected with thermography. While the active time needed to inspect this 8 m overlap joint is only 12 minutes, evaluating the thermography inspection data and manually repositioning the inspection jig can take significantly more time.

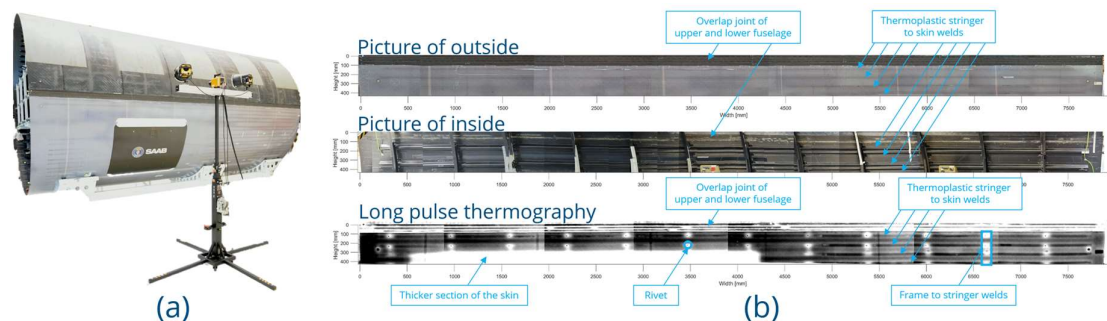


*Figure 15 Demonstration of NDT at large scale [15]. Thermography inspection of the overlap joint on the right hand side (RHS) of the Multifunctional Fuselage Demonstrator (MFFD) with (a) a picture of the set-up at Airbus ZAL, Hamburg, Germany, and (b) LPT inspection and corresponding pictures of the inside and outside.*

To address these challenges, NLR built a pilot automated inspection setup within the gantry at SAMXL, Delft, to inspect CFRP panels in the 8 m long by 4 m wide half-pipe fuselage assembly jig as part of the Penelope EU project, in which NLR, TU Delft and TNO participate among other partners. To simulate full-scale production, three panels were installed in the lower half-pipe fuselage assembly jig. Figure 16 shows a demonstration. The thermography inspection system can automatically scan any location in the jig and provide annotated results, which can be fed back into the digital production pipeline. This integrated setup enables rapid inspection of large parts, for example: a 50m<sup>2</sup> lower fuselage section can be inspected in just 1.5 hours, which is approximately 10 times faster than using Ultrasound C-scan, which would take around 14.5 hours.

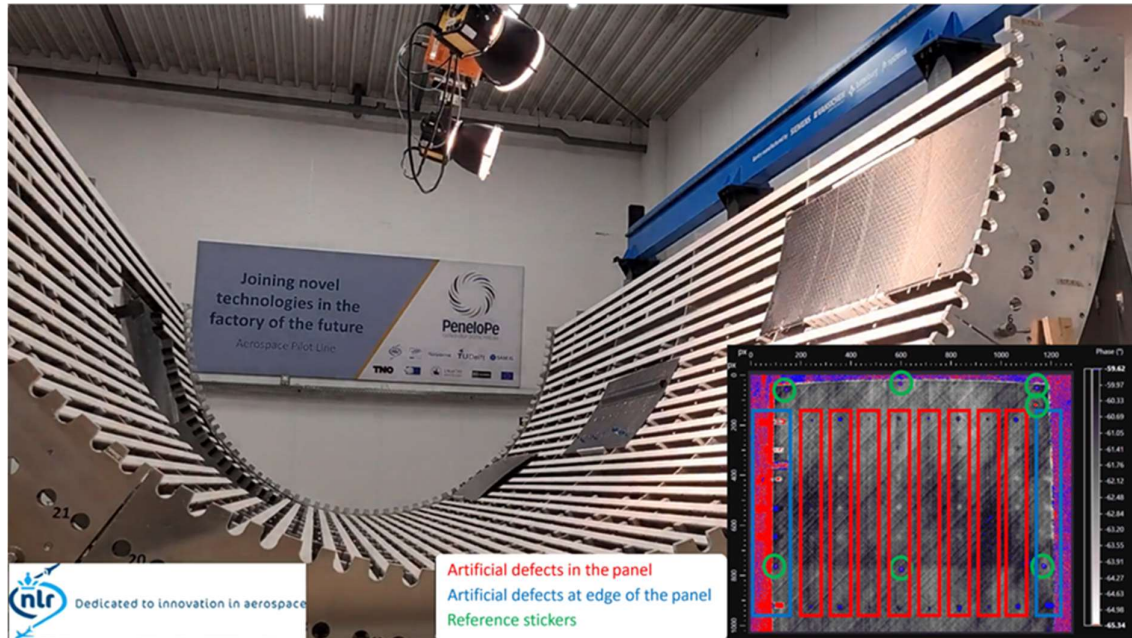


Figure 16 Demonstration of the automated large-scale thermography inspection in the assembly jig of the lower fuselage of the MFFD at SAMXL, Delft, with, in the lower right corner, an inserted thermography inspection result where artificial defects are highlighted in blue and red [15].

## 6.2. Development and evaluation of Laser Ultrasonic Inspection at NLR

Benjamin van Elburg, William Kramer, Jason Hwang, Jacco Platenkamp, Patrick Jansen (NLR)

Inspection of composite materials is time consuming work. While ultrasonic testing is excellent in defect detection, the alignment process is time consuming, the inspection speed is limited and the technique requires contact with the component through a coupling medium. For the national Groeifonds NXTGEN A programme NLR has developed a Laser Ultrasonic Inspection system that overcomes the disadvantages of traditional ultrasonic testing. The laser ultrasonic system is shown in Figure 17.



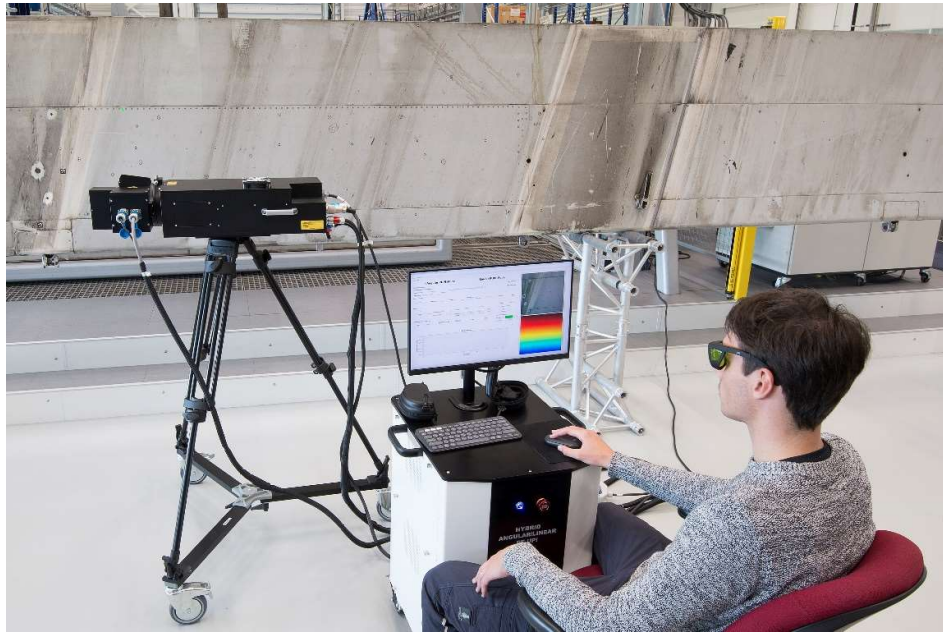


Figure 17 The laser ultrasonic inspection system scanning an aircraft component.

The laser system uses a pulsed laser to generate ultrasonic waves and a laser doppler vibrometer to detect the resulting vibrations. Mirrors allow for rapid translation of the test location at a maximum speed of 10 meter per second. By combining the laser ultrasonic system with a 3D scanner and rotation table the developed system is able to automatically scan curved components and map the results on a digital representation of the component, see Figure 18. Furthermore, the inspection time is up to 2 order of magnitude lower than traditional ultrasonic inspection.



Figure 18 A) The laser ultrasonic scanner. B) A curved CFRP component with markers on the inside. C) The rapid laser ultrasonic inspection. D) The inspection results mapped on a digital representation of the component

## 7. Structural Health & Usage Monitoring

### 7.1. SHM for LH2 tank applications

Frank Grooteman, Jan Willem Wiegman and Gerben van de Vrie (NLR)

Hydrogen-powered aircraft has become a topic of major interest in order to eliminate CO<sub>2</sub> emissions in aerospace (low carbon aviation). The development of Hydrogen has many unique properties that make it suitable for combustion, and nevertheless hydrogen (H<sub>2</sub>) for propulsion cannot yet be used in current transport aircraft.

A liquid hydrogen (LH<sub>2</sub>) fuel system has specific requirements and safety issues, such as measuring in-service conditions. An SHM system that monitors the health and safety of the LH<sub>2</sub> fuel system can play an important role in health and safety. A possible promising sensor technology is optical sensing, offering advantages over traditional sensors such as no EMI, no ignition source and no heat input.

At NLR several fibre optic sensors designed and manufactured by Somni Solutions for application in a LH<sub>2</sub> tank SHM system during filling and operation have been and are being thoroughly tested. These consist of a pressure sensor to measure the H<sub>2</sub> pressure inside the tank at various pressures and temperatures, a cryogenic temperature sensor to monitor the temperature inside the tank, a levelling sensor to measure the LH<sub>2</sub> level inside the tank, strain sensing at cryogenic conditions to monitor the load levels of the inner tank and an H<sub>2</sub> leak detection sensor to monitor for possible leakage at for instance appendages. An impression of two of these sensors and their output is given in Figure 19 and Figure 20.

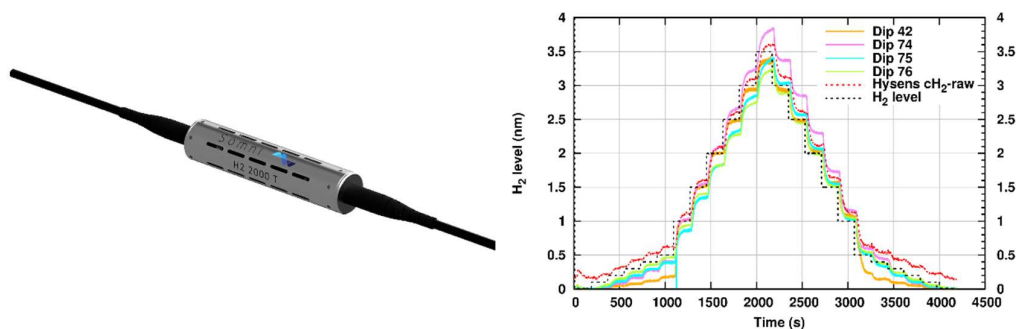


Figure 19 Somni H<sub>2</sub> leak detection sensor (left) and an example response measurement of a stepwise increase and decrease of H<sub>2</sub> levels (right)

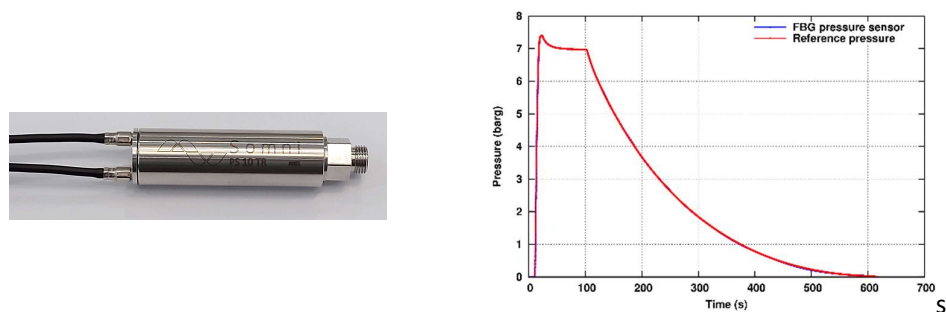
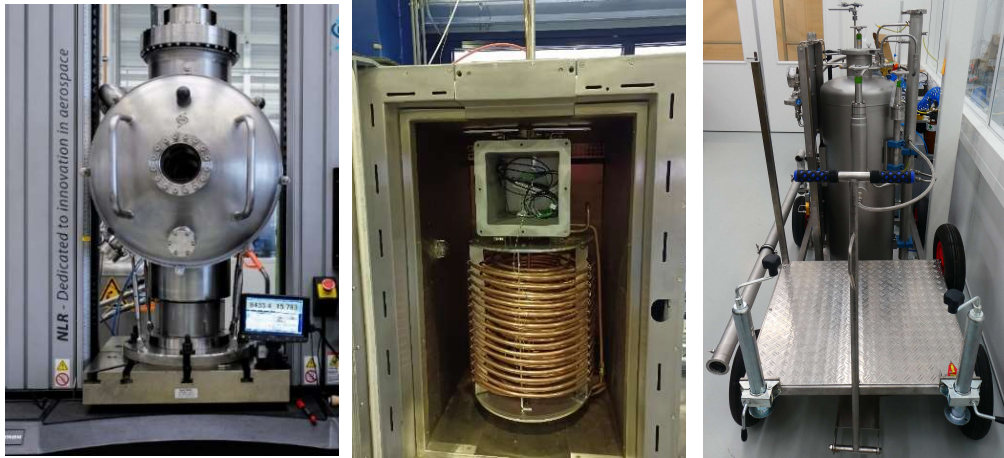


Figure 20 Somni GH<sub>2</sub> pressure sensor (left) and example pressure response measurement (right)

Dedicated (cryogenic) test facilities have been developed at NLR for this and other purposes, see Figure 21. With the cryostat test facility, material testing (static and limited cycling) can be performed at LH2 cryogenic conditions. With a H2 leak detection facility, the full range of H2 levels (0 to 100 %) can be tested at a wide range of temperatures (-150 to 350 °C) and pressures (up to 10 bar). With a LH2 bath cryostat test facility, various tests can be performed in a real LH2 environment such as, temperature, levelling and permeability testing.

The final goal is to demonstrate the fibre optic sensors in LH2 tank demonstrations at NLR.



*Figure 21 NLR test facilities to test SHM LH2 tank sensors, a cryostat (left), a H2 leak detection facility (middle) and a LH2 tank test facility LiHCA (right)*

## 8. Fleet Life Management

### 8.1. Individual tracking of RNLAF aircraft

*Marcel Bos (NLR)*

The Royal Netherlands Air Force (RNLAF) and NLR collaboratively keep track of the loads and usage of most aircraft types in the RNLAF inventory, viz. the F-16 Block 15, C-130H/H-30, NH90, AH-64E, ICH-47F, AS532 and F-35. This is done on an individual basis (individual aircraft tracking, IAT) and involves the installation of data acquisition and recording equipment, the development of modern data information systems and processing software, the development of fatigue and/or corrosion damage indices, the collection and processing of loads and usage data, the fusion of the collected usage data with the maintenance databases of the RNLAF to enable and enhance reliability analyse efforts, and the reporting of the processed data to the RNLAF. The results are used to:

- keep track of the consumed fatigue life;
- assess the severity of specific missions and mission types;
- evaluate and possibly optimize the usage of the fleets;
- optimize maintenance programs;
- assess/anticipate required structural modifications programs;
- provide the OEM with high-quality data in case of modification programs;
- rationalise decisions regarding tail number selection in the case of out-of-area deployment, fleet downsizing, decommissioning, etc.;
- develop load spectra for full-scale component testing;
- gain insight in the root causes of accidents and failures;
- enhance reliability analyses.

Many details of these programs were already supplied in previous National Reviews. A new activity is the development of a Fibre Optic Sensing-based IAT-program for the NH90 helicopter.



*Figure 22 NH90 helicopter of the RNLAF (from: NLR repository).*

## References

- [1] Amsterdam E, Wiegman JWE, Nawijn M, De Hosson JThM. On the strain energy release rate and fatigue crack growth rate in metallic alloys. *Engineering Fracture Mechanics* 2023;286:109292.
- [2] Amsterdam E, Nawijn M, Grooteman FP, Bos MJ. Variable amplitude fatigue life methodology for a structural digital twin. AVT-369 Digital Twin Technology Development and Application for Tri-Service Platforms and Systems, Båstad, Sweden: NATO Science & Technology Organization; 2023, p. 1–.
- [3] Koufis, S., Eskue, N., Zarouchas, D. et al. Monitoring the Cold Spray Process: Real-Time Particle Velocity Monitoring Through Airborne Acoustic Emission Analysis. *J Therm Spray Tech* 33, 2657–2671 (2024). <https://doi.org/10.1007/s11666-024-01878-1>
- [4] Van Ingen, J.W., Thermoplastic Orthogrid Fuselage Shell, *Sampe Journal* 52(5): 7-15, September (2016).
- [5] U.S. Department of Transportation, Federal Aviation Administration, Advisory Circular 20-107B, Change 1, Composite Aircraft Structure, August 24 (2010).
- [6] Biagini, D., Fatigue behavior of impacted carbon fibre reinforced plastics, PhD dissertation, Delft University of Technology. <https://resolver.tudelft.nl/uuid:09ac860d-dbf7-4d02-a750-8267afbdb26a>
- [7] Tu, W., Pascoe, J.A., Alderliesten, R.C. (2025), Comparison of mode II delamination behaviours in multidirectional and unidirectional composite laminates, *Comp Part B* 291, 111941. <https://doi.org/10.1016/j.compositesb.2024.111941>
- [8] Li, X., Monticeli, F.M., Pascoe, J.A., Mosleh, Y. (2024), Interlaminar fracture behaviour of emerging laminated-pultruded CFRP plates for wind turbine blades, *Engineering Fracture Mechanics* 308, 110353
- [9] Monticeli, F.M., Biagini, D., Mosleh, Y., Pascoe, J.A. (2025), A novel analytical model to characterise the monotonic and cyclic contribution of fibre bridging during Mode I fatigue delamination in (C)FRPs, *Composites Part B* 297, 112319
- [10] Leciñana, I., Renart, J., Turon, A., Zurbitu, J., Tijs, B.H.A.H. (2023), Characterization and analysis of the mode I interlaminar fatigue behaviour of thermoplastic composites considering curve effects, *Engineering Fracture Mechanics* 286, 109273.
- [11] Leciñana, I., Renart, J., Carreraas, L., A. Turon, J. Zurbitu, B.H.A.H. Tijs (2024), A fatigue test based on inclined loading block concept to benchmark delamination growth considering loading history and curve effect, *Composites Part A* 181, 108128.
- [12] Leciñana, I., Carreraas, L., Renart, J., Zurbitu, J., Tijs, B.H.A.H., Turon, A. (2024), A simulation strategy for fatigue modeling of delamination in composite structures under multiple loading conditions considering loading history and curve effects, *Composites Part A* 186, 108402.
- [13] Jansen, H.P.; Platenkamp, D.J.; Hwang, J. Hybrid Inspection Method using Three Dimensional Scanning, Lock-in Thermography and Laser Shearography. In *Proceedings of the WCNDT conference*, Seoul, South Korea, 27-31 May 2024. DOI: <https://doi.org/10.58286/29892>
- [14] Roth, Y.C.; Herrmann, R.; Sanchez Santos, C.; Uellendahl, M.; Koopman, J.; Henneberg, A.; Kos, J.; Villegas, I.F.; Choudhary, A.; Larsen, L.; Ferstl, S.; Diehl, B.; Emanuelsson, F.; Singhal, J.-B.; Pleth, M.; Atherton, K. CleanSky2/Clean Aviation large passenger aircraft for more sustainable commercial fuselage technologies – Major achievements. In *Proceedings of the ICAS conference*, Florence, Italy, 9-13 Sep. 2024.
- [15] Deutz, D. B., Bosch, A.F., Baptista, D.E., Van Veen, E.S., Platenkamp, D.J., Jansen, H.P. (2024), Non-contact NDT methods for large-scale CFRP aircraft parts. *Engineering proceedings* 6, under review.